Sensors and Materials, Vol. 34, No. 6 (2022) 2479–2491
MYU Tokyo

S & M 2984

Wearable Bracelet Using Radio Frequency Identification Tag with Antenna Directly Printed on Paper

Shang-Yeh Wen,[1] Cheng-Yu Peng,[2*] Ully Raihany,[2] and Cheng-Chien Kuo[1]

[1]Department of Electrical Engineering, National Taiwan University of Science and Technology, 43, Keelung Rd., Sec. 4, Da'an Dist., Taipei City 106335, Taiwan
[2]Department of Electronic Engineering, National Chin-Yi University of Technology, 57, Sec. 2, Zhongshan Rd., Taiping Dist., Taichung 411030, Taiwan

(Received December 31, 2021; accepted June 17, 2022)

Keywords: radio frequency identification tag, wearable bracelet, S-parameter, computer simulation technique software, direct printing on paper

We propose a method for printing a radio frequency identification (RFID) tag on paper as a sensor for a wearable bracelet via the Internet of Things (IoT) to allow people to enter a secure area. The RFID paper tag is first printed out when entering the area and then can be torn up by hand when leaving. It can be easily destroyed and cannot be used again, thus preventing privacy violations. This paper tag technology has a low cost, high confidentiality, and low environmental impact. Before using RFID in this manner, it was first necessary to develop an appropriate antenna for use with the RFID tag. In this study, computer simulation software was used to select the best antenna from seven samples that matched the predetermined frequency requirements and obtain S-parameters that matched the desired frequency (924 MHz). This antenna can be used for a removable RFID tag printed directly on a wearable paper bracelet. Reliability experiments were conducted with printed antennas for RFID tags printed directly on paper. This wearable bracelet device can be easily removed to ensure personal security and has industrial applications combining RFID and the IoT.

1. Introduction to RFID Application

Radio frequency identification (RFID) is currently applied in various areas of daily life. RFID is widely used to facilitate personal, commercial, and industrial activities. An RFID tag uses a sensor or transponder to retrieve and store data remotely for identification purposes using radio waves, labels, or ordinary RFID cards attached to a product, an animal, or even a human.(1) An RFID tag comprises a silicon microchip and antenna and contains electronically stored information. It can be read from up to several meters away if it passes through an RFID reader, depending on the frequency and power used in the regulatory standards for RFID. RFID is used as a sensor for Internet of Things (IoT) systems, where sensors can be applied to identify objects, collect data, or supervise individual targets. RFID collects information through sensing systems, peripheral components, and embedded systems and transmits sensor signals via the internet.

*Corresponding author: e-mail: peng@ncut.edu.tw
https://doi.org/10.18494/SAM3797

ISSN 0914-4935 © MYU K.K.

Therefore, people or machines can analyze the collected data and make decisions on the basis of the results. Mutual communication and collaboration enable the easy realization of Industry 4.0 applications, including smart cyber-physical systems and smart factories, using IoT software and hardware.

The European Parliament passed a bill on March 28, 2019, by 560 votes to 35 votes, stipulating that EU countries will completely ban the use of single-use plastic products, including RFID electronic tags, from 2021. Medical units in various regions have used RFID in many applications. Therefore, in this paper, we propose a smart RFID paper tag and epidemic prevention management system that uses a paper substrate as an electronic tag, without the use of polyethylene terephthalate (PET), which can satisfy the 2021 EU disposable plastic requirements. This smart technology can provide important results in relation to the prevention of the COVID-19 pandemic, for which IoT application is an important technology. Currently, all RFID electronic tags use PET substrates, and viruses can survive for a long time on PET when they are worn in high-risk environments. In addition, the policy of Ministry of Health and Welfare of Taiwan stated that the medical waste treatment method for plastic substrates is obsolete and may cause environmental pollution if used extensively. Therefore, using a paper substrate as an anti-epidemic tag has the advantages of a short virus survival time and incineration after its use. The COVID-19 pandemic has led to smart medical developments that effectively use the health insurance system and digital technology to assist the prevention of epidemics; however, for this purpose, the use of personal data will become increasingly necessary. The personal information obtained by data application must be confidential and eventually deleted. This aspect is still not considered in the laws and regulations of some countries, and a hidden risk of privacy infringement persists.

Viruses exhibit a shorter survival time on the surface of an RFID paper tag than on PET. Paper tags can reduce the likelihood of hospital equipment and environmental items becoming potential disease vectors. The National Institutes of Health (NIH) published the survival times of viruses on the surfaces of different materials, as listed in Table 1.[(2)] They concluded that the survival time on cardboard or a mobile phone case was longest, and the survival time on a plastic or stainless steel surface was third among the materials investigated. This showed that hospital equipment and environmental items are potential media for disease. NIH tested seven materials that are commonly found in homes and hospitals by spreading the virus on a surface and leaving it to incubate for periods of several hours to days. Thereafter, the surface of the material was wiped and it was investigated whether the virus could still be cultured in a Petri dish.

Table 1
Survival times of viruses on the surfaces of different materials.[(2)]

	HCoV-19 Half-life (h)			SARS-CoV-1 Half-life (h)			HCov-19 – SARS-CoV-1 difference (h)		
Material	Median	2.5%	97.5%	Median	2.5%	97.5%	Median	2.5%	97.5%
Cardboard	8.45	5.95	12.4	1.74	0.827	4.42	6.6	3.07	10.7
Plastic	15.9	13	19.2	17.7	14.8	21.5	−1.79	−6.31	2.51
Aerosols	2.74	1.65	7.24	2.74	1.81	5.45	−0.00418	−2.72	4.45
Copper	3.4	2.4	5.11	3.76	2.43	5.43	−0.321	−2.31	1.78
Steel	13.1	10.5	16.1	9.77	7.69	12.3	3.36	−0.173	7.12

In this study, an RFID paper tag was proposed for use as a wearable bracelet to allow all people with wearable bracelets to enter a secure area of a hospital while monitoring personnel movement. Paper tags have a low cost and low environmental impact, and the tags can easily be destroyed to avoid privacy violations. Everyone entering the hospital can wear an RFID paper tag on their wristband, similar to obtaining a license plate for a car. Moreover, the device can be printed directly on a paper substrate. General printers can be used to print out health insurance or personal information on this wearable RFID bracelet. The RFID paper tag can first be printed out when entering the hospital and then be torn up by hand when leaving. It can be easily destroyed, preventing its reuse and the possibility of preventing privacy violations.

In RFID antenna simulations for a high-sensitivity sensor, Ariff *et al.*[3] examined a miniature design for a Minkowski order-3 fractal nesting slot patch antenna for an RFID passive tag at 5.8 GHz with the impedance aligned with that of the tag chip. They used particle swarm optimization to fit the compact and broadband area antenna. This miniature design used the computer simulation technique (CST). Microwave Studio (MWS) electromagnetic (EM) software was used as a simulator to design a miniature fractal antenna with an impedance that perfectly matched that of the tag chip. Tan and Ismail[4] designed an antenna operating at 919–923 MHz, which is allocated for ultrahigh-frequency (UHF) RFID systems in Malaysia. The resulting parameters, namely, antenna radiation, gain, bandwidth, return loss, and voltage wave ratio, were investigated by antenna simulation with CST Studio Suite 2013 based on finite integral techniques with an antenna size of 130 mm × 120 mm × 1.6 mm^3. Kunze *et al.*[5] described the design of a UHF tag antenna that operated within the regulated frequency range of Malaysia (919–923 MHz) using a 3D EM field in CST MWS as a simulator. The radiation antenna operated at 919.5 MHz in the H and E fields, making it a suitable sensor for general use in the environment. Similar to the studies cited above,[4,5] which used CST software in antenna design simulation, Hassouni and Qjidaa performed simulations in the CST Studio Suite.[6] The high-performance 3D EM software package was used to design, analyze, and optimize EM components and systems. EM field breakers for applications across the EM spectrum are included in a single user interface in the CST Studio Suite to determine whether the created RFID antenna is optimal and conforms with the established rules.

As examples of RFID sensor and IoT applications, Ali and Yusoff[7] presented a monitoring method for individuals entering a room using a small-scale prototype built to test the concept of an RFID-photocell system comprising an RFID, two photocells, an Arduino, and a PLX-DAQ tool. The attendance-taking process began when tagged participants passed through the range of an RFID reader, where their tag code was compared with a database. If the database could match the code, the participant's information, such as their name, ID number, date, and time, was displayed in an Excel file. Forkan *et al.*[8] focused on monitoring and assessing worker productivity. This research using the Industrial Internet of Things (IIoT) is especially important for large manufacturing plants where most production activities are conducted by workers using tools and operating machines. This IIoT solution captures accelerated and gyroscopic data from wearable sensors on edge computers and analyzes them on powerful processing servers in the cloud to provide timely performance and productivity evaluations of each individual worker on the production line. Huang and Lu[9] focused on the job performance of subcontractor workers in

the construction industry, which plays an important role in determining the quality of construction projects. Several demographic variables, such as age, education, number of children, and pay, affect job performance and deserve the attention of managers. The results of their study provide insights into the performance of construction workers and can serve as a basis for improving worker performance to ensure a sufficient workforce. Ahmed *et al.*[10] stated that the skills of a workforce significantly impact the time, cost, and quality of a construction project. To check the status of workers, they set nine key parameters for worker skills. This research was conducted using a questionnaire designed on the basis of a very in-depth literature review and expert opinions, which was distributed among construction workers in Bangladesh to determine the quality of their work.

Industry 4.0 combines technology and automation, and collaboration is required between a company and industry players. Peng *et al.*[11] performed sound detection to obtain the main frequency and amplitude of a CNC machine during production and designed a detection program using the LabVIEW program to determine whether it was running well. Sheng[12] introduced an acquisition and analysis system using the LabVIEW program to obtain the signal generated by a signal generator and analyzed it by setting two acquisition frequencies of 2 and 20 kHz. It was experimentally found that the standard error generated at 2 kHz was greater than that generated at 20 kHz. The LabVIEW program was designed to work well, and a simulation was conducted to determine worker performance using RFID technology.[13]

In this study, we propose a wearable RFID tag on a patient's wristband that is directly printed on paper on the basis of RFID substrate research. We considered seven RFID antennas with different shapes and sizes using Sonnet software, and their parameters were adjusted. These parameters were then imported into the CST software to observe the frequency response and determine whether it was close to the desired regulatory standards. This research required a few changes in the physical and geometric parameters, such as the length and thickness, to achieve high performance for the RFID tag. The proposed geometric structure for the RFID tag allowed a greater range than that of conventional tags. After the geometry of the antenna was changed, the S-parameter results were obtained for the desired range regulation, namely, the US 902–928 MHz range.[14] This experiment showed that the fourth of the seven antennas exhibited the best results. This antenna was used for a removable RFID tag on a wearable bracelet by printing the RFID antenna directly on paper.

2. Printing RFID Antennas Directly on Paper

2.1 Antennas designed using CST simulation software

Seven types of antennas with different dimensions and geometries were obtained from the printing production line, as shown in Fig. 1. These antennas had dimensions of 50.00 × 20.00 mm^2 (Type-1), 54.63 × 15.00 mm^2 (Type-2), 50.00 × 15.00 mm^2 (Type-3), 61.0 × 10.00 mm^2 (Type-4), 70.00 × 15.00 mm^2 (Type-5), 70.99 × 9.00 mm^2 (Type-6), and 27.00 × 10.00 mm^2 (Type-7). These antennas were manufactured from silver and used a Ucode 8 IC, and the frequency range used in the simulation was 800–1000 MHz.

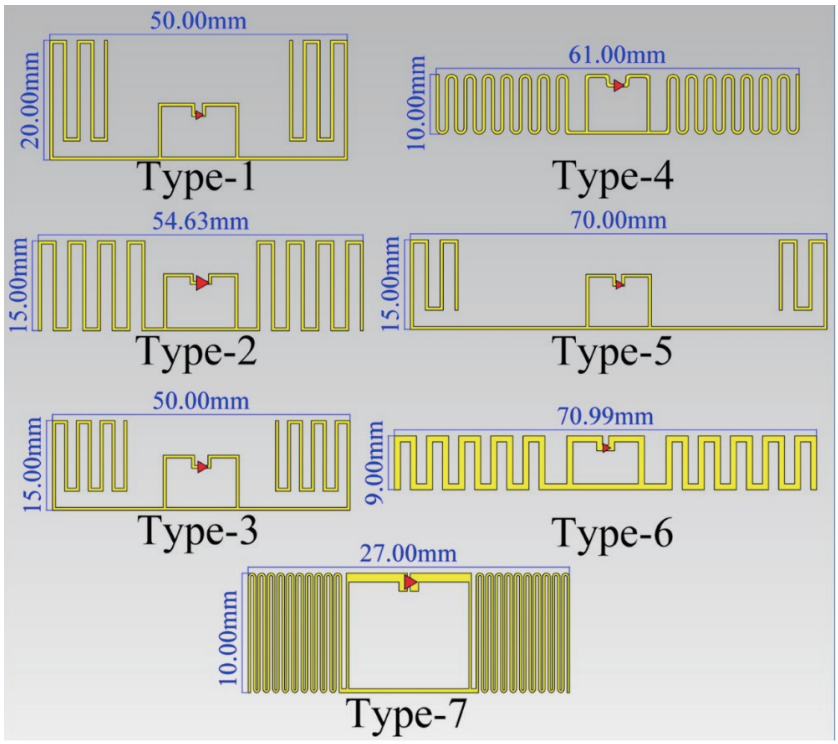

Fig. 1. (Color online) Seven samples with designed antennas.

The designed parameters of the antennas were not only the dimensions and geometries; the substrate was also a key factor. The simulation method used the antenna design of Type-5 but with both corrugated and plastic substrates. Figure 2 shows the different values for the read range and center frequency of different substrates in a curved field. The RFID antenna had to be redesigned to satisfy the requirement of a curved field, and the CST EM simulation software was used for analysis and simulation of the RFID antenna.

The antennas had a discrete port on each side of the RFID circuit and an impedance of 50 Ω. The voltage standing wave ratio (VSWR) in the CST software was simulated by using a matching structure for impedance matching with 50 Ω between the antenna and the reference transmission feed line.[15] For a given VSWR related to the RFID circuit in this study, the value was for the range of UHF frequencies. Usually, the VSWR is less than two for most antenna applications; however, it ranges from 1 to ∞, depending on the frequency of interest.[16] The time-domain solver is applied for the parameters used to start data retrieval.

2.2 Easily removable RFID tag

The flowchart in Fig. 3 shows the experimental process. Simulation experiments were conducted for the seven types of antennas using the CST software with the time-domain solver settings for the process.

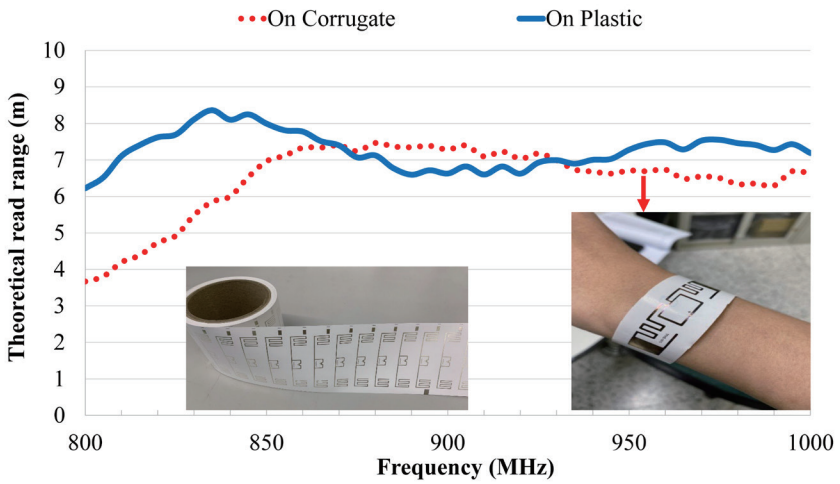

Fig. 2. (Color online) Different values of reading range and center frequency in curved field.

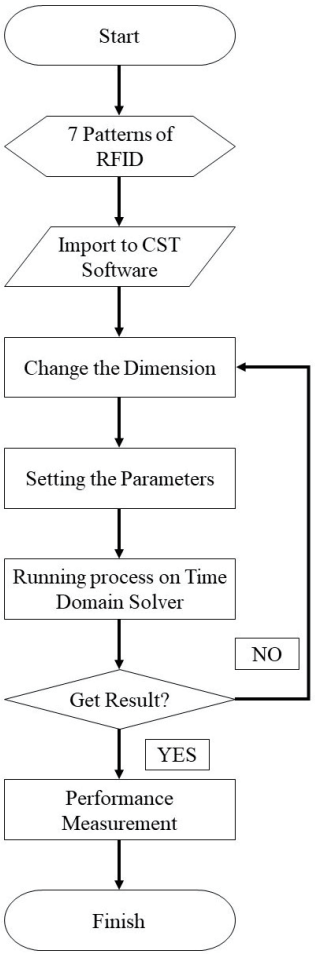

Fig. 3. (Color online) Flowchart of implementation for designed antennas.

3. Various Properties of Printed RFID Antennas

3.1 Impedance matching for RFID tag

An RFID antenna design is required for different application fields of epidemic prevention. After designing the wearable RFID bracelet with a curved field, the EM simulation software was used for RFID antenna analysis and simulation. The simulation software was used to build an antenna model of EM waves and analyze the frequency response to establish a geometric antenna to determine how the frequency response is related to the antenna power, gain, wavelength, and distance. The following equations are used in the analysis:

$$Z_c = R_c + jX_c\,, \tag{1}$$

$$Z_a = R_a + jX_a\,, \tag{2}$$

where Z_c and Z_a represent the complex impedances of the chip and antenna with real parts R_c and R_a and imaginary parts jX_c and jX_a, respectively.[17,18]

Here, S is the power density of an EM wave incident to the RFID tag antenna in free space given as[19]

$$S = \frac{P_t G_t}{4\pi r^2}\,, \tag{3}$$

where P_t is the transmitted power, G_t is the gain of the transmitting antenna, and r is the distance to the tag.

The power collected on the tag antenna, P_a, is defined as the maximum power that can be delivered at a suitable load in complex conjugations:

$$P_a = SA_e\,, \tag{4}$$

where A_e is the effective area of the antenna. A_e can be determined as

$$A_e = \frac{\lambda^2}{4\pi} G\,, \tag{5}$$

where G is the tag antenna gain.

3.2 Shape characteristics of RFID tag

Our first experiment was performed to demonstrate that our simulation was realistic by comparing the samples for which results had already been obtained and redesigning the antenna

using the printing production line in the CST software. The parameters are the dimension and the geometry (61.00 × 10.00 mm^2; Type-4), as shown in Fig. 4.

An RFID device with an antenna directly printed on paper was produced by the roll-to-roll printing with a nanosilver antenna (61 × 10 mm^2) using a Ucode 7 IC manufactured by NXP with a frequency range of 860–960 MHz. This section shows how the example was reproduced by simulating the RFID antenna provided. According to the result of Fig. 4, the peak frequency at 882 MHz was tuned to a frequency of 910 MHz, as shown in Fig. 5.

3.3 Selecting the best RFID antenna

After the simulation was run and all S-parameter results were combined into a single figure, the best antenna was found to be Type-4 because the lowest value of the S11 (return loss) curve was in the frequency band. As shown in Fig. 6, Type-4 had the desired center frequency, namely, 924 MHz , which is included in the US 902–928 MHz range.

4. Performances of RFID Antennas

4.1 Frequency variations for different substrates in design of Type-4 antenna

This section shows how the Type-4 RFID antenna was used in experiments with different substrate materials (air, paper, and plastic). As shown in Fig. 7, different RFID substrates had

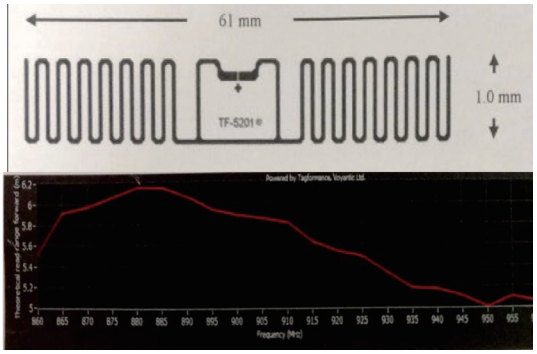

Fig. 4. (Color online) Shape characteristic and read range results.

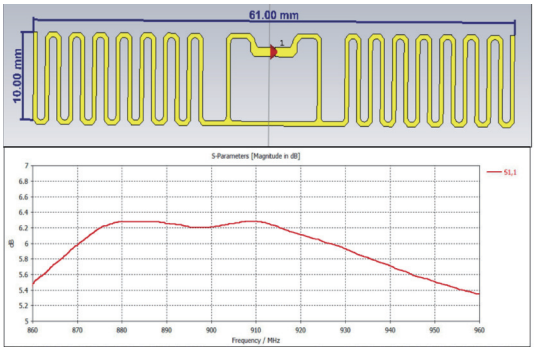

Fig. 5. (Color online) Shape characteristic after replacement and simulation results.

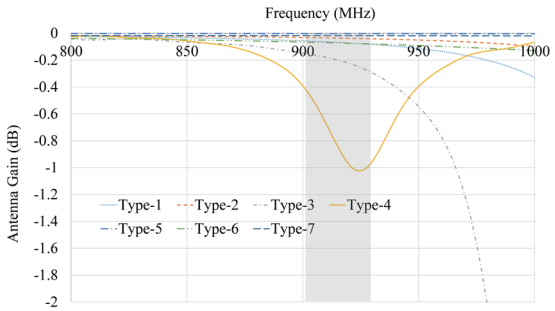

Fig. 6. (Color online) Antenna gain versus frequency for different antennas.

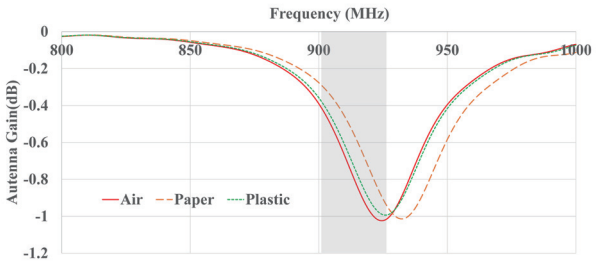

Fig. 7. (Color online) Center frequencies for different RFID substrates.

different center frequencies, affecting the read range. When the substrate of the Type-4 antenna was paper, the center frequency was outside of the desired range of 902–928 MHz (the minima of the curves for air, paper, and plastic substrates were located at 924, 932, and 926 MHz, respectively).

4.2 Printing RFID antenna directly on paper

For wearable RFID bracelets applied in curved fields, the available antenna power is a function of various factors, such as the transmitter power, gain, distance, and EM wavelength. The different geometries included curved surfaces, and the design improved the read range and gain without increasing the transmitter power, which was affected by different factors, including the center frequency and read range of the wearable RFID curved surface design. As shown in Fig. 8, a Voyantic Tagformance Pro tester (Espoo, Finland) was used for the field measurements of the RFID curved surface at 0° and 30° under the printing conditions of uniformity, insufficient ink, length, width, and resistance. At 920 MHz, the read ranges were 9.1 and 8.4 m at angles of 0° and 30°, respectively, and the change in the read range was less than 7.7%.

All process conditions during the disinfection of medical items were monitored using an RFID tag reader system with an RFID reader (ZEBRA FX7500, Lincolnshire, Illinois, United States) and linear antenna (gain: 8.5 dB, 902–928 MHz). The temperature information, time, and tag identifier (TID) were recorded during disinfection. The RFID measurement satisfied the upper limit of the disinfection temperature index (85 °C) for the RFID antenna materials, paper substrate, and accessories. Figure 9 shows the performance degradation in the reliability test at a high temperature of 85 °C and humidity of 85%, which resulted in a read range difference of 1.8% (average read ranges of 8.80 and 8.64 before and after the test, respectively).

4.3 Waterproof function of RFID sensor provided by plastic cover encapsulation

Figure 10 shows the RFID sensing performances for a printed RFID tag and packaging cover comprising a plastic film. The printed RFID tag also had an antenna printed on a paper substrate. The weight of a single printing RFID tag was 0.246 g. The printed RFID tag was then packaged

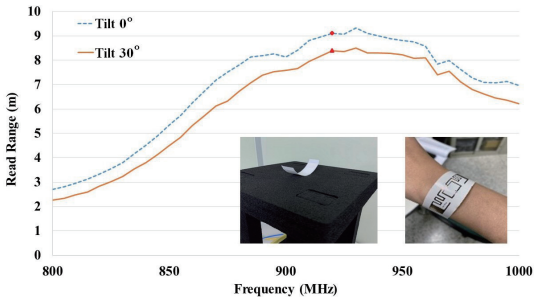

Fig. 8. (Color online) Wearable RFID bracelets applied in curved fields at 0 and 30°.

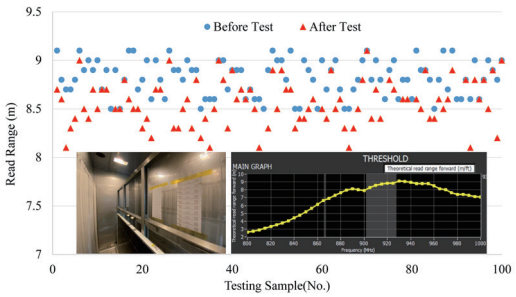

Fig. 9. (Color online) Results of reliability test of RFID paper tags at a high temperature of 85 °C and humidity of 85%.

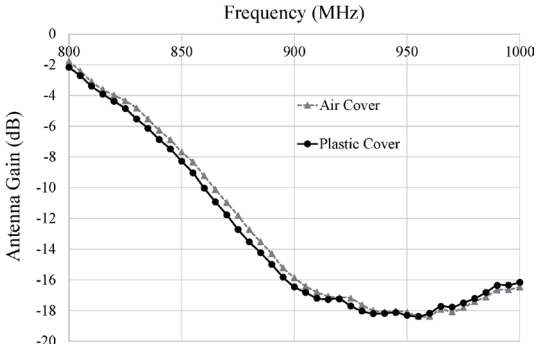

Fig. 10. RFID sensing performances for air cover and plastic cover.

using a thermal pressing process, where the cover of the packaging film had a three-layer structure (EVA/PE/PET) with the EVA side attached to the RFID tag. This three-layer structure had a thickness of approximately 0.08 mm and was fully transparent. The processing temperature of the thermal packaging was 140 °C, and the weight after packaging was 0.394 g. It was observed that the frequency at 924 MHz had the highest intensity. The RFID printed paper and its plastic film packaging had similar center wavelengths.

The uniform water spraying method was used in a waterproof test of the printed RFID tag. Water was sprayed with a sprinkler device at a distance of approximately 0.4 m from the RFID tag sample, and the results of the waterproof test were obtained with water droplets on the tag surface. The tag was directly covered and sprayed multiple times with various quantities of water droplets. The results in Fig. 11 show that only 0.08 g of water caused the intensity to decrease and the frequency to shift to a smaller value. When the weight of the sprayed water droplets exceeded 0.127 g, it was difficult to read the RFID intensity signal. Thus, the properties of printed RFID tags were susceptible to surface water droplets.

Therefore, the surface of the printed RFID tag was encapsulated using a film with a three-layer structure of EVA/PE/PET, and different quantities of water droplets were applied on the surface of the packaged tag to directly test the waterproofing. Spraying multiple times showed that the RFID tag could maintain the signal intensity within the read range when the amount of sprayed water reached 0.129 g (Fig. 12). When the amount of sprayed water reached 0.288 g, the

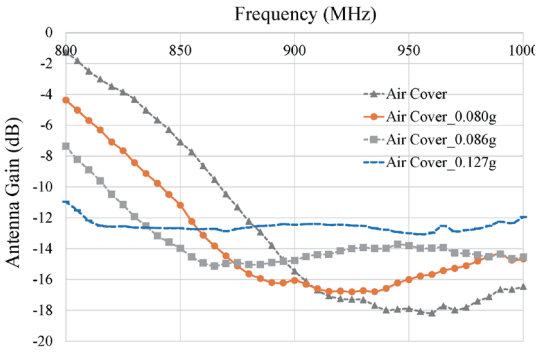

Fig. 11. (Color online) RFID sensing performance versus weight of water sprayed on air cover.

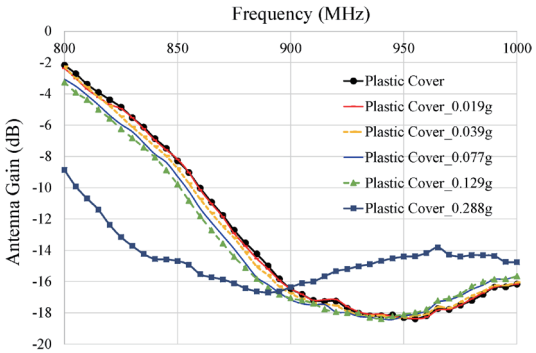

Fig. 12. (Color online) RFID sensing performance versus weight of water sprayed on plastic cover.

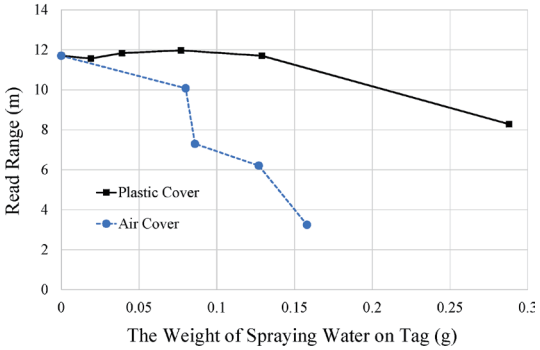

Fig. 13. (Color online) Read range versus weight of water sprayed on air and plastic covers.

frequency began to decrease. Thus, the packaging cover improved the waterproof characteristics of the printed RFID tag.

Figure 13 shows the read range characteristics of RFID tags with and without the packaging cover. The RFID tag with the plastic packaging cover maintained its sensing characteristics and therefore had the more waterproof performance, maintaining a read distance larger than 10 m. However, the RFID tag without a packing cover showed a rapid decrease in the read range. When the water droplet weight was approximately 0.158 g, the read range decreased to 3.247 m.

5. Conclusions

In this study, CST software was used to simulate the best RFID antenna chosen from seven samples obtained from a printing production line. The best results were obtained for the Type-4 antenna with an S-parameter of 924 MHz, which lies within the US standard range of 902–928 MHz. This antenna was redesigned to verify that the experimental and simulation results were similar, thus confirming the accuracy of the simulation. Finally, the substrate material was changed to air, paper, and plastic to determine the difference in the resulting return loss. The

RFID tag with a plastic packaging cover maintained its sensing characteristics and exhibited the most waterproof performance. Finally, a removable RFID tag was applied to a wearable bracelet by directly printing it on paper.

Acknowledgments

This research was funded by the Taiwan Ministry of Science and Technology under grant number MOST 110–2637-E-167–006. We would like to thank Smooth & Sharp Corporation for their support with the RFID production line and Industrial Technology Research Institute for their support with instrumentation and measurement.

References

1 J. Aliasgari, M. Forouzandeh, and N. Karmakar: IEEE J. Radio Freq. Identif. (RFID) **4** (2020) 146. https://doi.org/10.1109/JRFID.2020.2982822
2 N. V. Doremalen, D. H. Morris, M. G. Holbrook, A. Gamble, B. N. Williamson, A. Tamin, J. L. Harcourt, N. J. Thornburg, S. I. Gerber, J. O. Lloyd-Smith, E. de Wit, and V. J. Munster: N. Engl. J. Med. **382** (2020) 1564. https://doi.org/10.1056/NEJMc2004973
3 M. H. Ariff, I. Ismarani, and N. Shamsuddin: 2015 IEEE 6th Control and System Graduate Research Colloquium (IEEE, 2015) 61–65. https://doi.org/10.1109/ICSGRC.2015.7412465
4 C. L. Tan and W. Ismail: IEICE Proceedings Series (IEICE, 2011) 1–16. https://doi.org/10.34385/proc.53.FrP1–16
5 M. Kunze, Z. Reznicek, I. Munteanu, P. Tobola, and F. Wolfheimer: 2011 Int. Conf. Electromagnetics in Advanced Applications (IEEE, 2011) 110–113.
6 S. Hassouni and H. Qjidaa: 2014 Int. Conf. Multimedia Computing and Systems (IEEE, 2014) 1314–1317.
7 M. A. H. Ali and N. A. Yusoff: 2018 IEEE Int. Conf. Automatic Control and Intelligent Systems (IEEE, 2018) 83–88.
8 A. R. M. Forkan, F. Montori, D. Georgakopoulos, P. P. Jayaraman, A. Yavari, and A. Morshed: 2019 IEEE 39th Int. Conf. Distributed Computing Systems (IEEE, 2019) 1393–1403.
9 Y.-H. Huang and K.-W. Lu: First Int. Technology Management Conf. (IEEE, 2011) 315–317.
10 S. Ahmed, H. Islam, I. Hoque, and M. Hossain: Int. J. Construct. Manage. **20** (2020) 480. https://doi.org/10.1080/15623599.2018.1487158
11 C. Y. Peng, U. Raihany, S. W. Kuo, and Y. Z. Chen: Sensors **21** (2021) 4288. https://doi.org/10.3390/s21134288
12 Z. Y. Sheng: 2016 IEEE Advanced Information Management, Communicates, Electronic and Automation Control Conf. (IEEE, 2016) 330–334.
13 A. Sharif, Y. Yan, J. Ouyang, H. T. Chattha, K. Arshad, K. Assaleh, A. A. Alotabi, T. Althobaiti, N. Ramzan, Q. H. Abbasi, and M. A. Imran: Electronics **10** (2021) 1603. https://doi.org/10.3390/electronics10131603
14 Z. Hameed and K. Moez: Microelectron. J. **62** (2017) 49.
15 F. Majeed and D. V. Thiel: Int. J. Antennas Propag. (2016) 7398567. https://doi.org/10.1155/2016/7398567
16 M. Shahpari, D. V. Thiel, and A. Lewis: IEEE Trans. Antennas Propag. **62** (2014) 950. http://doi.org/10.1109/TAP.2013.2290794
17 M. Dhaouadi, M. Mabrouk, T. P. Vuong, D. Hamzaoui and A. Ghazel: 7th European Conference on Antennas and Propagation (EuCAP) (2013) 3056–3059.
18 P. Nikitin, J. Kim, and KVS Rao: (2021) IEEE International Symposium on Antennas and Propagation and USNC-URSI Radio Science Meeting (APS/URSI) 167–168. http://doi.org/10.1109/APS/URSI47566.2021.9704608
19 Y. Amin, Y. Feng, Q. Chen, L. R. Zheng and H. Tenhunen: IEICE Electronics Express **10** (2013) 1. https://doi.org/10.1587/elex.10.20130003

About the Authors

Shang-Yeh Wen received his B.S. degree from the Department of Electro-Optical Engineering, Minghsin University of Science and Technology, Taiwan, and his M.S. degree in electrical engineering from Yuan Ze University, Taiwan. He is currently pursuing his Ph.D. degree with National Taiwan University of Science and Technology. He is also working at the Industrial Technology Research Institute as an engineer. His research interests include electro-optical technology, photovoltaic systems, and power systems. (d10707010@mail.ntust.edu.tw)

Cheng-Yu Peng received his Ph.D. degree from the Graduate Institute of Mechanical and Electrical Engineering, National Taipei University of Technology, Taiwan, in 2007. He is currently an assistant professor in the Department of Electronic Engineering, National Chin-Yi University of Technology. Before that, he was a researcher at the Industrial Technology Research Institute. His current research interests primarily involve smart sensors and supervisory control, intelligent robotics, opto-electrical precision measurement, automation and mechatronics, solar energy, and engineering applications. (peng@ncut.edu.tw)

Ully Raihany was born in Indonesia in 1997 and received her B.A.S. degree in telecommunication engineering from the Electrical Engineering Department, State Polytechnic of Sriwijaya, Indonesia, in 2019. She is currently studying for her master's degree in electronic engineering at National Chin-Yi University Technology, Taiwan. She is a member of the ICT Laboratory, and her research interests are RFID and sound detection.
(4a813033@gm.student.ncut.edu.tw)

Cheng-Chien Kuo received his B.S., M.S., and Ph.D. degrees from National Taiwan University of Science and Technology (NTUST) in 1991, 1993, and 1998, respectively. He was with St. John's University from 1994 to 2015. In 2015, he joined NTUST, where he is currently a professor and the chairman of the Department of Electrical Engineering. His research interests include fault diagnosis, conditional monitoring system design, distribution automation, partial discharge measurement, and optimization techniques. (cckuo@mail.ntust.edu.tw)